Large Eddy Simulation and Proper Orthogonal Decomposition of the Flow in Annular Channels

Project Representative

Hisashi Ninokata   Nuclear Engineering Department, Graduate School of Engineering and Science, Tokyo Institute of Technology

Authors

Elia Merzari   Nuclear Engineering Department, Graduate School of Engineering and Science, Tokyo Institute of Technology

Hisashi Ninokata   Nuclear Engineering Department, Graduate School of Engineering and Science, Tokyo Institute of Technology

LES (Large Eddy Simulation) numerical methodology has been used to fully reproduce the characteristics of the flow field in eccentric annular channels, to verify and characterize the presence of large-scale coherent structures, to examine their behavior at different Reynolds numbers and to characterize the anisotropy associated to these structures. The numerical approach is based upon boundary fitted coordinates and a fractional step algorithm; a dynamic Sub-Grid Scale (SGS) model suited for this numerical environment has been implemented and tested. The agreement with previous experimental and DNS results has been found good overall for the streamwise velocity, shear stress and the rms of the velocity components. The instantaneous flow field presented large scale coherent structures in the streamwise direction at low Reynolds numbers, while these are absent or less dominant at higher Reynolds. The effect of secondary flows on anisotropy is studied over an extensive velocity range through invariant analysis. Additional insight on the mechanics of turbulence in this geometry is obtained though POD (Proper Orthogonal Decomposition) of the flow filed.

Keywords: LES, POD, Eccentric channel, Advanced Nuclear Systems, Tight Lattice

1. Introduction

A major objective of this research is to establish a computational simulation-based design and safety approach in nuclear engineering, in particular in the area of nuclear fuel pin subassembly thermal hydraulics design and safety. Emphasis is placed on the delineation, in-depth understanding and modeling of the complex turbulent flow structure inside nuclear fuel pin subassemblies characterized by non-homogeneous and anisotropic turbulence. Applications of Direct Numerical Simulation of turbulence and Large Eddy Simulation techniques are fully employed being aimed at providing higher quality of computational data that should be equivalent to or more detailed information than those provided by experimentation. Also the computational results will be used for engineering modeling as well as the basis on which design data base is constructed.

Calculations have been carried out for the eccentric annulus channel flows as a simplified geometry in connection to the turbulent flows in tight lattice nuclear fuel pin subassemblies. Eccentric annular pipe flows represent an ideal model for investigating inhomogeneous turbulent shear flows, where conditions of turbulence production vary significantly within the cross-section. Moreover recent works have proven that in geometries characterized by the presence of a narrow gap, large-scale coherent structures are present. The eccentric annular channel represents, in the opinion of the present authors, the prototype of these geometries. There, influences of the anisotropic turbulence structure and eddy migration behaviors in the non-uniform flow channels will be investigated in detail.

2. Methodology

In previous research several DNS computations have been performed for the concentric and eccentric channels. The data collected has been used to evaluate different SGS model in order to develop an effective LES methodology in boundary fitted coordinates.

The Navier-Stokes equations have been solved in boundary fitted coordinates ([1], [2]):

$$\frac{\partial \overline{u_i}}{\partial t} + \frac{\partial (\overline{U_k}\,\overline{u_i})}{\partial \xi_k} = -\frac{\partial}{\partial \xi_k}\left(\left(\frac{\overline{J^{-1}\,\overline{\xi_{kj}}\,\overline{p}}}{\rho}\,\delta_{ij} + T_{ik}\right)\right) + v\frac{\partial}{\partial \xi_k}\left(\overline{J}^{-1}\,\overline{g_{kl}}\,\frac{\partial \overline{u_i}}{\partial \xi_l}\right),$$

(1)

$$\frac{\partial \bar{J}^{-1} \overline{\xi_{ki} u_i}}{\partial \xi_k} = 0, \tag{2}$$

where J is the Jacobian, g denotes the skewness tensor, and:

$$T_{ik} = \overline{U_k u_i} - \overline{U_k}\,\overline{u_i}, \tag{3}$$

$$U_k = J^{-1} \xi_{jk} u_j, \tag{4}$$

$$\xi_{ij} = \frac{\partial \xi_i}{\partial x_j}. \tag{5}$$

Where gij represents the skewness tensor, ξ_i is the boundary fitted coordinate in the i-th direction and u_i is the the cartesian velocity coordinate in the i-th direction. T_{ik} represents the Sub-Grid scales stress tensor than need to be modeled. An *a priori* analysis as well as an *a posteriori* analysis of the flow in concentric annuli and eccentric annuli has been carried out to evaluate possible models.

Several models have been tested, among which, the dynamic Smagorinsky, the dynamic mixed model, the self-similarity model and another variants of the dynamic model ([3]).

The dynamic model and its variant performed fairly well from the point of view of *a priori* and *a posteriori* tests. They may be considered the ideal choice for the simulation of the flow in annular channels and rod-bundles.

The algorithm used to solve the Navier-Stokes equations is based on the Fractional Step Algorithm on a partially non-staggered grid ([4]). Equation (1) has been discrtized through a second order consistent scheme ([5]) and Time advancement has been carried out through an Adams-Bashfort scheme. The Poisson equation for the pressure gauge has been solved with an FFT solver since perioidc boundary conditions have been employed in the streamwise direction.

3. Results

An extensive LES computational campaign has been performed for the eccentric channel at different values of Reynolds number and the eccentricity to investigate the characteristics of the flow in eccentric channels. All the cases run are summarized in Table 1 for different values of the geometric parameters D_h (hydraulic diameter), α and e:

$$\alpha = \frac{D_{in}}{D_{out}}, \tag{6}$$

$$e = \frac{d}{D_{out} - D_{in}}. \tag{7}$$

Where D_{in} and D_{out} are the inner and outer diameters and d is the distance between the axis of the two cylinders. The results of the simulations A, B and D (see Table 1) have been validated to available DNS and experimental data ([6], [7], [8]).

Important aspects of the flow field in concentric and eccentric annuli have been confirmed and reproduced through the present methodology ([9]). In particular, the effect of transverse curvature on the inner wall, as well as the effect of eccentricity on the wall shear stress, has been successfully simulated. Contour plots show the effect of the parameter α (Fig. 1) and the eccentricity (Fig. 2). Moreover, some fundamental observations have revealed that:

1. flows in eccentric annuli are characterized by a strong Reynolds effect in the narrow gap in the Reynolds region surveyed;
2. flows in eccentric annuli present secondary flows, whose shape is constant in the range of Reynolds number surveyed but depends upon the value of eccentricity (an example of secondary flows is given in Fig. 3 for $\alpha = 0.3$ and e = 0.5);
3. at low Reynolds numbers the secondary flows are associated to coherent periodic structures in the direction of homogeneous turbulence, the flow is characterized by

Table 1 LES cases

	e	α	D_h [m]	$1/\nu$ [s]	Re	Grid N_ξ- N_η- N_z	L [m]	Time weeks
Case A	0.0	0.1	1	540	8800	128-64-128	5	4
Case B	0.5	0.5	1	250	3200	256-64-(128-512)	$2\pi,4\pi,8\pi$	8
Case C	0.5	0.5	1	770	12100	256-128-(128-256)	$2\pi,4\pi$	8
Case D	0.5	0.5	1	1480	27100	512-300-512	2π	20
Case E	0.8	0.5	1	250	3100	256-64-128	2π	8
Case F	0.8	0.5	1	750	11300	256-128-128	2π	8
Case G	0.95	0.5	1	500	8700	256-64-128	2π	8
Case H	0.5	0.3	1	250	2900	256-64-128	2π	8
Case I	0.5	0.7	1	250	3300	256-64-128	2π	8

high coherence lengths;

4. the condition of anisotropy of turbulence in the narrow gap changes greatly as the Reynolds number increases; and

5. for a constant eccentricity and hydraulic diameter, if α increases the spanwise distribution of the streamwise velocity is increasingly inhomogeneous (Fig. 1).

From previous works and the evidence presented here it appears that the transition to turbulence in eccentric annuli is accompanied by the formation of a street of counter-rotating vortices in the region near the narrow gap. These coherent structures (Fig. 4) persist at low Reynolds numbers but they progressively become less dominant, at least for an eccen-

tricity equal to 0.5, as the Reynolds number increases.

In the narrow gap the local profile of the streamwise velocity evolves from a purely laminar solution to a solution characterized by the presence of turbulence production near walls.

The flow develops very slowly toward fully developed turbulent flow (for Re = 27100 and e = 0.5 the streamwise velocity profile does not follow the law of the wall in the narrow gap region).

The process of transition is apparent from Fig. 5 that shows the shear stress in the narrow gap region for cases C and D. It is evident that at low Reynolds numbers the shear is considerably lower and the peaks are shifted toward the center of the channel. For case B, the shear stress is nearly
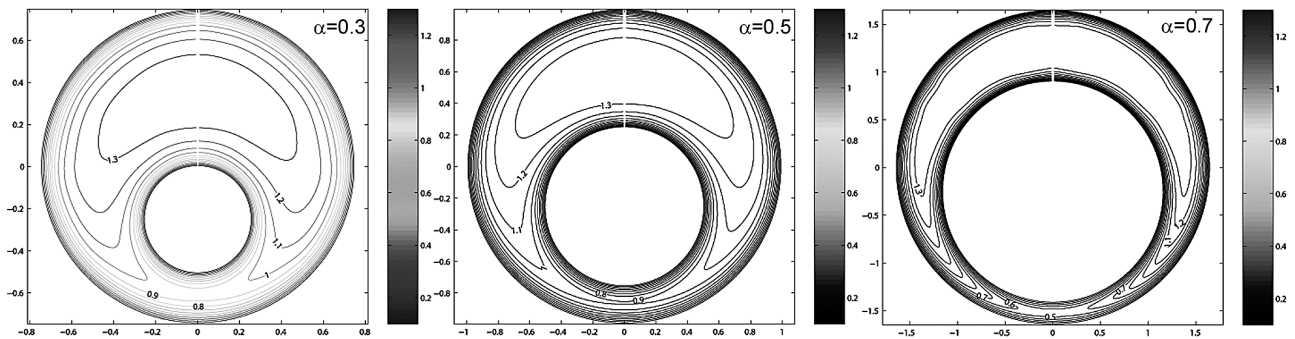

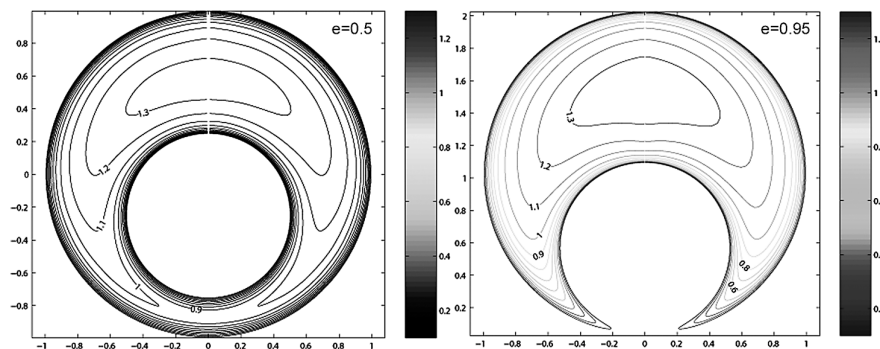Fig. 1 Effect of inner to outer diameter ratio on the streamwise velocity distribution.

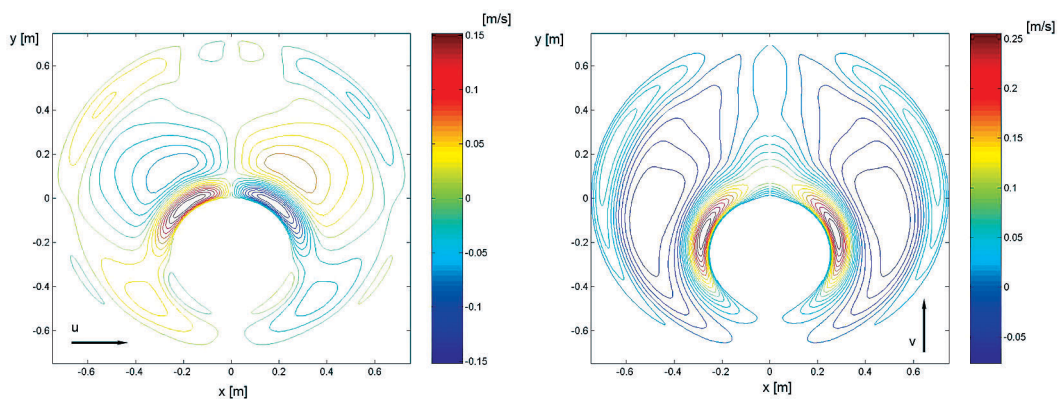Fig. 2 Effect of eccentricity on the streamwise velocity distribution.

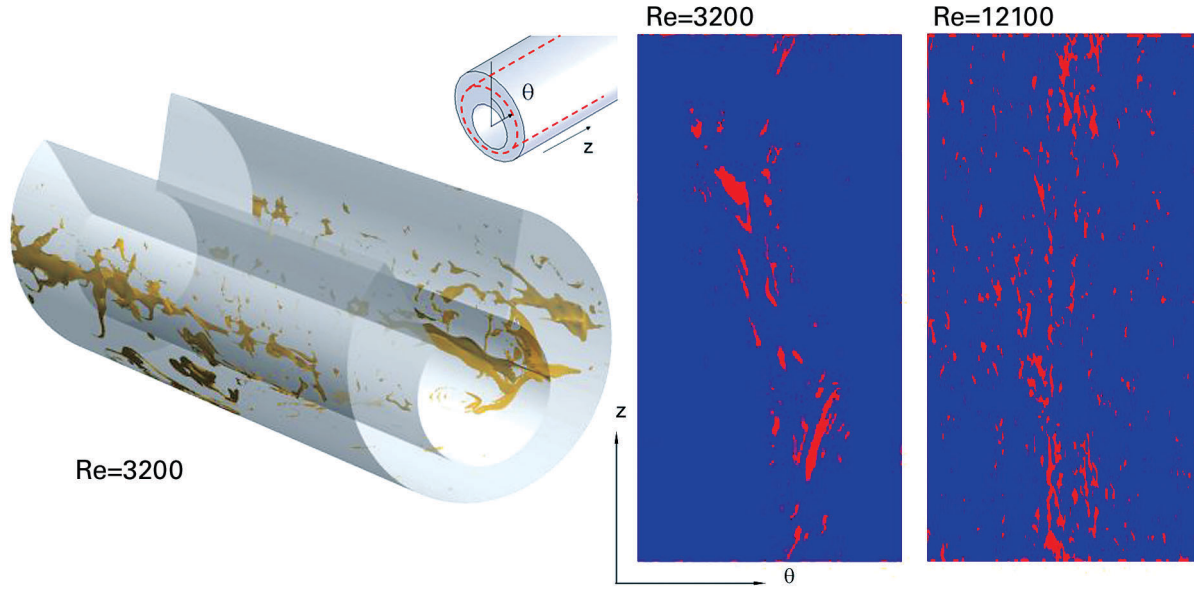Fig. 3 Secondary flows for e = 0.5, α = 0.3 and Re = 3150.

271

Fig. 4 Iso-surface for the second invariant of the velocity tensor at Q = 0.8 for a Reynolds number of 3200 (left),
contour plot at the same value for a Reynolds number of 3200 and in the gap mid-section (right).

zero in the narrow gap region, indication that turbulence production is negligible in the area and that turbulence is only transported. In conclusion, at e = 0.5, the shear stress in the narrow gap region evolves from an almost laminar condition for a Reynolds number equal to 3200 to an increasingly turbulent solution for cases C and D.

At low Reynolds number and for eccentricity equal to 0.5 the relative dominance of the coherent structures is associated with a strong anisotropy in the narrow gap (turbulence has a local two-component pattern), while at higher Reynolds numbers a nearly isotropic condition is recovered far from the walls. At higher values of eccentricity (0.8) the structures persist to be dominant even at Reynolds as high as 11300, and anisotropy continues to be dominant in the narrow gap. At even higher eccentricity (e = 0.95) the coherent structures are absent in the narrow gap region, accounting
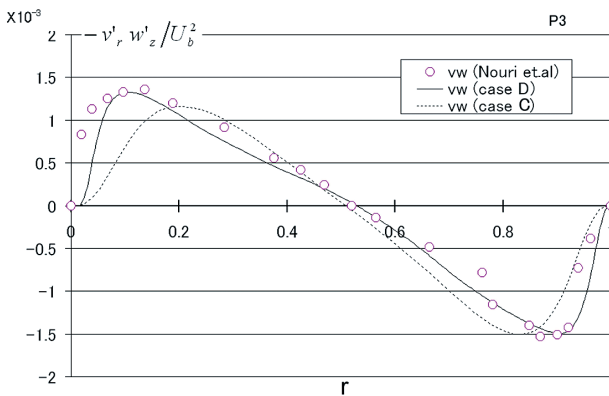

Fig. 5 Shear Stress distribution (normalized by the square of the bulk velocity) as a function of the relative distance from the outer wall in the narrow gap.

for a strong viscous damping effect in the case of almost touching channels.

It appears that transition to fully developed turbulence in the narrow gap is delayed at eccentricity equal to 0.8 if compared to an eccentricity equal to 0.5. In general the delay in transition between the flow in the wide gap region and the narrow gap region depends upon the eccentricity.

3.1 Proper Orthogonal Decomposition

A POD (Proper Orthogonal Decomposition) study ([10]) for the turbulent fields calculated in this study has been performed to obtain an additional insight in the physics of flow in eccentric channels. The power of the POD lies in the fact that the decomposition $\vec{\sigma}_i(\vec{x})$ of the flow field in the POD eigen-functions:

$$\vec{u'(x)} = \sum_i a_i \vec{\sigma}_i \vec{(x)} \tag{8}$$

(where a_i are real coefficients) converges optimally fast in L_2; i.e. a truncation of n modes in the POD decomposition is the optimal possible truncation for the same number of modes. Each mode is characterized by its energy content; the rank of the modes based on their energy content will be called "quantum number" in the following. Detailed description of the procedure used can be found in Sirovich ([11], [12], [13]).

The POD has been carried out at two Reynolds numbers (Re = 3200 with a domain length of 4π and Re = 12100 with a domain length equal to 2π) at e = 0.5 with 2000 snapshots each. The case with lower Reynolds number shows that the first 6 modes contain 20% of the total energy while at higher Reynolds number the 6 most energetic modes contain

approximately 6% of the total energy. This indicates that an energy transfer occurs between the most energetic modes and the other modes (Fig. 6).

The first four modes in the case with Re = 3200 and the first two modes in the case at Re = 12100 are representative of a traveling wave of the type $\vec{u} = \vec{u}_0 \sin\left(2\pi\left[\frac{x}{\lambda} - \frac{t}{T}\right]\right)$, which can in fact be split into two contributions:

$$\vec{u} = \vec{u}_0 \sin\left(\frac{2\pi}{\lambda}x\right)\sin\left(\frac{2\pi}{T}t + \frac{\pi}{2}\right)$$
$$-\vec{u}_0 \sin\left(\frac{2\pi}{\lambda}x + \frac{\pi}{2}\right)\sin\left(\frac{2\pi}{T}t\right)$$

(9)

where the two terms differ in the axial direction x by a phase shift of π/2. Figure 7a shows one of the two modes representative of the two terms in equation (9), at Re = 3200.

For the case at Re = 3200 two wavelengths appear to be present. In fact the use of periodic boundary conditions and a finite computational length in the streamwise direction imply a discretized wavenumber spectra and subsequently the impossibility for the computation to reproduce exactly the correct wavenumber spectrum (unless the domain is extremely long, in the sense discussed in [14]). These issues are discussed extensively in Merzari et al. ([14]). For Re = 3200, the modes corresponding to quantum numbers m = 4 and m = 5 contain a series of vortexes on the edges of the gap (Fig. 7).

4. Conclusions

Evidence based on this and previous research suggests that in eccentric channels coherent structures are present for some combination of the geometric parameters and Reynolds number.

The POD conducted on eccentric channels shows that the coherent structures are associated to traveling-wave modes. For e = 0.5 and α = 0.5, they are considerably less energetic as the Reynolds increases, and they appear to be less dominant toward other modes. However, for other combination of

the geometric parameters e and a, a similar effect might not be observed, in particular for higher eccentricity where, for e = 0.8, the coherent structures are resilient up to Re = 11300.

Anisotropy conditions in the narrow gap also depend upon the value of the geometric parameters and Reynolds number. In particular, higher value of eccentricity imply that a strong anisotropy persist in the narrow gap even at higher Reynolds numbers (as high as 11300 for eccentricity of 0.8).

References

[1] Jordan S.A., "A Large Eddy simulation methodology in generalized curvilinear coordinates", *Journal of Computational Physics*, **Vol.148**, pp.322–340 (1999).

[2] Jordan S.A., "Dynamic Subgrid-Scale Modeling for Large-Eddy Simulations in Complex Topologies", *Journal of Fluids Engineering*, **Vol.123**, 3, pp.619–627 (2001).

[3] Merzari E., Ninokata H., "Test of LES SGS models for the flow in annular channels", Proceedings of ICAPP 2007, Nice, France, 13–18 May 2007.

[4] Y. Zang; R. L. Street, J.R. Koseff, "A non-staggered grid, fractional step method for time-dependent incompressible Navier-Stokes equations in curvilinear coordinates", *Journal of Computational Physics*, **Vol.114**, p.1 (1994).

[5] Suzuki T., Kawamura N., "Consistency of Finite - Difference Scheme in Direct Simulation of Turbulence", *Trans. JSME*, **Vol.60**, pp.578 (1994) (in Japanese).

[6] Nikitin N.V., "Direct Numerical Simulation of turbulent flows in eccentric pipes", *Computational Mathematics and Mathematical Physics*, **Vol.46**, pp.509–526 (2006).

[7] Nouri J. M., Umur H. and Whitelaw J. H., "Flow of Newtonian and non-Newtonian fluids in concentric and eccentric annuli", *Journal of Fluid Mechanics*, **vol.253**, pp.617–64, (1993).

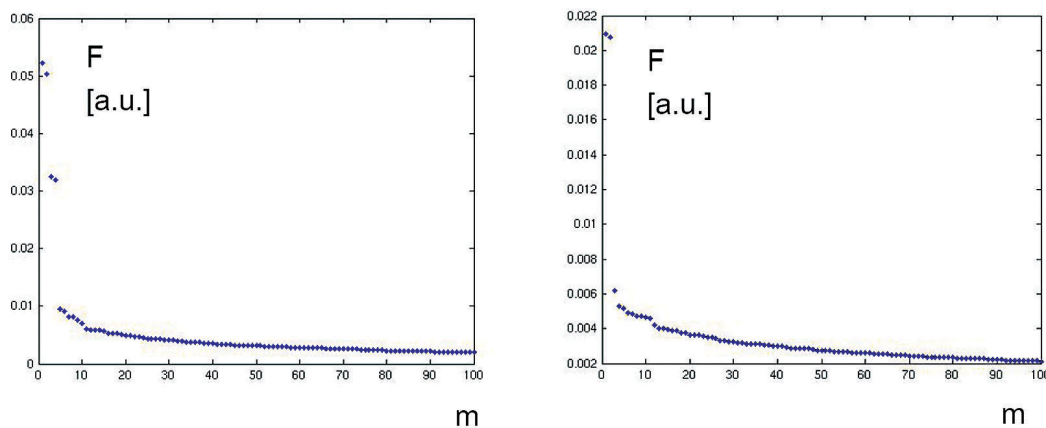[8] Chung S.Y., Rhee G. H., Sung H., "Direct numerical simulation of turbulent concentric annular pipe flow

Fig. 6 Eccentric channel: energy distribution of the principal modes of the POD decomposition, Re = 3200 and Re = 12100.
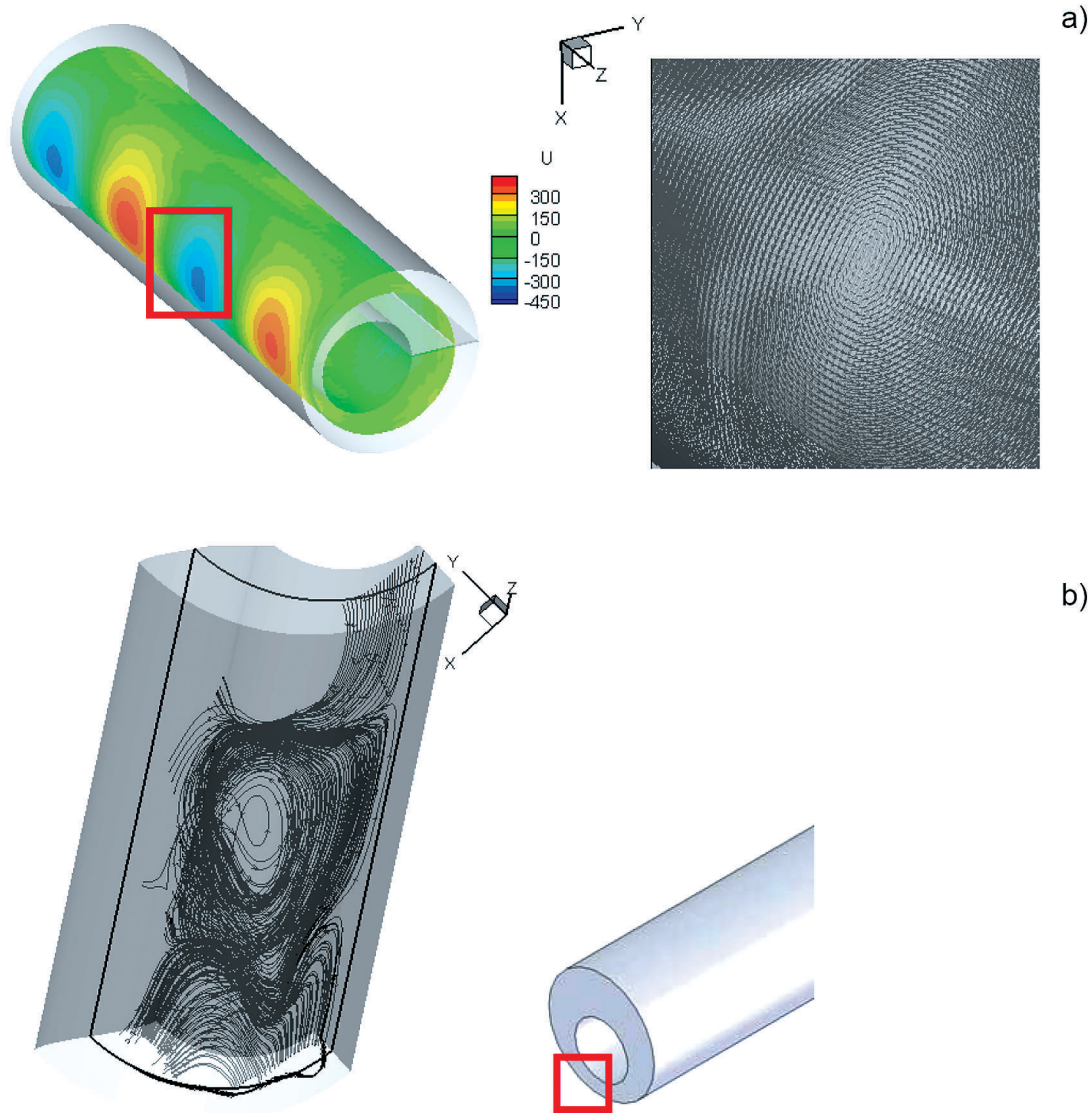
a)

b)

Fig. 7 Most energetic mode, normalization arbitrary, Re = 3200. Streamlines for the mode with quantum number, m = 6, Re = 3200.

Part 1: Flow field", *International Journal of Heat and Fluid Flow*, **vol.23**, pp.426–440, (2002).

 [9] E. Merzari and H. Ninokata, "Anisotropy and Coherent Structures in Eccentric Annular Channels, Flow, *Turbulence and Combustion* (accepted with minor revisions).

[10] G. Berkooz, P. Holmes, J.L., Lumley, The proper orthogonal decomposition in the analisys of turbulent flow, *Annual Reviews of Fluid Mechanics*, **25**, pp.539–575 (1993).

[11] L. Sirovich, Turbulence and the dynamics of coherent structures, Part I: Coherent structures, *Quarterly of Applied mathematics*, **XLV**, pp.561–571 (1987).

[12] L. Sirovich, Turbulence and the dynamics of coherent structures, Part II: Symmetries and transformations, *Quarterly of Applied mathematics*, **XLV**, pp.573–582 (1987).

[13] L. Sirovich, Turbulence and the dynamics of coherent structures, Part III: Dynamics and scaling, *Quarterly of Applied mathematics*, **XLV**, pp.583–590, (1987).

[14] E. Merzari, H. Ninokata and E. Baglietto, "Numerical Simulation of the Flow in Tight-Lattice Fuel Bundles", *Nuclear Engineering and Design* (in press, available online).

LESによる二重円環流路内の乱流計算とPODによる分析
(Large Eddy Simulation and Proper Orthogonal Decomposition of the Flow in Annular Channels)

プロジェクト責任者
二ノ方　寿　　東京工業大学　大学院理工学研究科　原子核工学専攻

著者
Elia Merzari　　東京工業大学　大学院理工学研究科　原子核工学専攻
二ノ方　寿　　東京工業大学　大学院理工学研究科　原子核工学専攻

　本研究の目的は、流路チャンネルが複雑で実験計測上取得困難な乱流特性などを高い信頼性の裏づけをもった直接乱流シミュレーション（DNS）および大渦シミュレーション（LES）によって提供し、現象の解明を実施するとともに現象の機構論的なモデル化を行って工学的な応用に有効に活用することである。

　複雑形状流路の典型である高速炉または低減速型軽水炉炉心における稠密格子配列型燃料集合体サブチャンネル内の乱流構造のRe数依存性や配列格子のピッチ対燃料直径比に対する依存性は現象論的に極めて複雑である。その現象解明を行うには計算科学的手法が唯一の手段と考えられる。稠密格子燃料集合体内サブチャンネル内の乱流は、燃料要素間隔が狭いために壁の影響を強く受け、非等方性が強い。一般的に燃料集合体内の乱流は、P/Dの減少およびRe数が低くなると燃料間隙部近傍でその非均質性が増すとともに、局所的な乱流−層流遷移領域を含み、流れそのものが不安定となることが予測される。

　本稿は、燃料集合体より簡略な流路形状である偏心二重円環流路内における十分に発達した乱流を対象として実施した境界適合型座標系上のLESによる主流方向流れの時間平均流速分布、せん断応力、各揺らぎ成分のRMSなどについて、これまでに得られている直接乱流シミュレーション結果および実験データと比較して十分な精度で一致していることの確認とともに、流路形状の非一様性から生じる二次流れによって輸送される乱流渦の動的な挙動と主流方向における大局的な流れとの相互作用、これらの流路形状とRe数依存性の解明に関する報告である。とくに低Re数条件下では、狭隘ギャップ部における層流と乱流の遷移現象、軸方向スパンに見た大局的な乱流場におけるコヒーレントな振動モードの発現を同定するとともに、高Re数領域においては等方的な乱流場へ移行し、こうした局所的な乱流−層流遷移現象および大局的な振動現象が消滅することを明らかにした。また、膨大な三次元時間依存の乱流計算結果の図形処理のみでは埋もれてしまう可能性がある物理情報の抽出に、POD (Proper Orthogonal Decomposition) を適用して複雑な乱流構造の動的な挙動を客観的に示すことにより、流動様式間の遷移、局所および大局の流れの振動モードのメカニズムを説明することができた。こうした偏心円環流路に代表される非一様幾何形状流路内乱流挙動に関する知見は、原子炉炉心稠密格子配列燃料集合体流路内乱流場にも十分適用できるものと考えられ、今後、こうした地球シミュレータによる乱流計算を原子炉燃料集合体流路内乱流解析へ適用し、燃料集合体設計データベースを計算科学的手法によって構築していく予定である。

キーワード：LES，POD，偏心二重円環流路，稠密格子，新型原子炉